Multi-rate track-following control with robust stability for a dual-stage multi-sensing servo system in HDDs

Ryozo Nagamune, Xinghui Huang, and Roberto Horowitz

Department of Mechanical Engineering

University of California, Berkeley, CA 94720-1740

{ryozo,xhhuang,horowitz}@me.berkeley.edu

Abstract

This paper proposes a multi-rate design method for robust track-following controllers in hard disk drives (HDDs). The HDDs to be considered are dual-stage multi-sensing systems. A track-following problem, which takes into account robust stability, is formulated as a periodically time-varying version of the standard mixed H_2/H_∞ control problem. This problem is solved via the solution of linear matrix inequalities. Simulation results show that multi-rate controllers can achieve much better track-following performance than single-rate controllers, while achieving the same guaranteed robust stability margin.

Key Words: Dual-stage servo, track-following control, multi-rate control, robust stability, periodically time-varying systems.

1 Introduction

The capacity of hard disk drives (HDDs) heavily depends on track density. As track density increases, more precise track-following control of the magnetic read/write head is required. Conventional single-stage servo systems, which utilize a voice coil

motor (VCM) as an actuator and the position error signal (PES) as a measurement, have serious limitations that prevent them from achieving the high track-following performance required for next generation HDDs. It is expected that *dual-stage multi-sensing (DSMS) servo systems*, which incorporate additional actuators and sensors, may be able to satisfy these high performance requirements [10, 8].

In a DSMS servo system, a digital controller needs to be designed. Its inputs are the position of the read/write head relative to the center of the data track, known in the HDD industry as the PES, and other measurements, which may include outputs of vibration sensors and position of the read/write head relative to the suspension tip. Its outputs are control signals to the VCM and a piggy back microactuator. Among these controller input/output signals, only the sampling rate of the PES is predetermined by the fixed disk spinning speed and the fixed number of servo sectors allotted on the disk. On the other hand, sampling rates of other signals have no such restrictions. Therefore, those rates can be made faster than that of the PES [7], in order to take full advantage of the ability of the DSMS system. In this way, the design of a DSMS servo system boils down to a *multi-rate multivariable control problem*.

The main control objective in track-following is to obtain a small RMS value of the PES against all undesirable exogenous disturbance such as track runout, windage and measurement noise. This objective has to be attained by a single controller for a huge batch of disks with slightly different dynamics. As a consequence, the track-following controller should be designed in a *robust* manner.

There are several previous researches for robust/multi-rate track-following controller design. In [6], multi-rate track-following control is considered for single-stage single-sensing systems. For single-sensing systems, multi-rateness is not an issue mathematically in the design, since the lifting technique does not cause the so-called "causality constraint" (see for example [1]). Also, in [6], the H_∞ norm is used

as a performance criterion. However, the H_2 norm is more appropriate to be used as a measure for tracking performance. The H_2 norm was used for track-following controller design of single-stage single-sensing systems in [15], with robust stability. Several multi-rate robust controller design techniques for DSMS systems have been presented, for example, in [10, 8]. However, these techniques are not "optimal", in the sense that the design is divided into several steps, which are individually optimal but may not be optimal as a whole.

In this paper, we propose a new design method of track-following controllers in HDDs for DSMS systems. The method is based on a multi-rate multivariable control synthesis, and takes robustness into consideration to some extent. As a secondary actuator, we utilize a MEMS microactuator (MA) which is located between the suspension tip and the slider. Moreover, as additional sensors, we propose the use of both strain sensors fabricated on the suspension for sensing the suspension vibration, and a capacitive sensor integrated in the MA for sensing the slider motion relative to the suspension. For a multi-rate system, a track-following control problem with adequate robust stability margin is formulated as a periodically time-varying version of the mixed H_2/H_∞ control problem. We will apply the techniques for analysis and synthesis for time-varying systems in [3, 13] to this problem, and solve it with linear matrix inequalities (LMIs) ([4, 14, 5]).

The paper is organized as follows. In Section 2, the DSMS system to be dealt with in this paper is explained in detail. Section 3 mathematically formulates a robust multi-rate track-following problem. This problem is reduced to a standard mixed H_2/H_∞ control problem to be solved via LMIs. The LMIs and the controller construction from the LMI variables are presented in Appendix. Section 4 demonstrates the efficiency of the designed multi-rate robust controller with computer simulations.

2 Dual-stage multi-sensing servo system

In this section, we will explain the dual-stage multi-sensing system to be dealt with in the subsequent sections. The block diagram of the system is depicted in Figure 1. All the notation used in the figure will be explained in this section, and used throughout the paper.

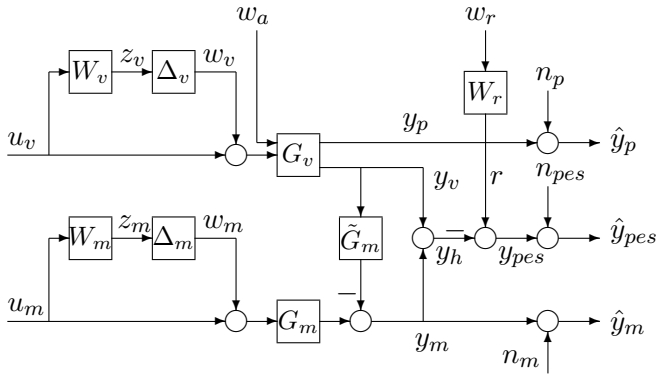

Figure 1: Block diagram of a dual-stage multi-sensing system

2.1 Voice Coil Motor (VCM)

The mechanical components of the track-following servo system in a conventional HDD include a voice coil motor (VCM), an E-block, a suspension and a slider. The slider is supported by the suspension and flies over the surface of disk on an air bearing. The magnetic read/write head is fabricated on the edge of the slider. The VCM actuates the suspension with the slider about a pivot in the center of the E-block. The control input of this system is the voltage input to the VCM, while the measurement output is the position error signal (PES) of the head, relative to the disk data track center. For convenience, we will refer to this dynamics simply as the VCM dynamics.

The input-output relation of the VCM plant is assumed to be expressed in the

frequency domain by

$$\begin{bmatrix} y_p(s) \\ y_v(s) \end{bmatrix} = G_v(s) \begin{bmatrix} I & 0 \\ 0 & 1 + W_v(s)\Delta_v(s) \end{bmatrix} \begin{bmatrix} w_a(s) \\ u_v(s) \end{bmatrix}. \tag{1}$$

Here, inputs are the airflow turbulence w_a and the current u_v in the VCM, and outputs are the generated head motion y_v and the suspension vibration y_p which is caused by w_a and will be sensed by a PZT sensor instrumented on the suspension. The disturbance w_a is assumed to be white noise with Gaussian distribution. The nominal model for the VCM is assumed to be given by

$$G_v(s) := \frac{A_0}{s^2} + \sum_{i=1}^{6} \frac{A_i}{s^2 + \zeta_i \omega_i s + \omega_i^2}, \tag{2}$$

where A_i, ζ_i and ω_i are respectively constant gain matrices, damping ratios and natural frequencies. In addition, the transfer function from u_v to $[y_p, y_v]^T$ is assumed to have dynamic uncertainty $W_v\Delta_v$, where $\|\Delta\|_\infty \leq 1$ and W_v is a weighting function. Finally, the auxiliary variables (z_v, w_v), which are the input and the output of Δ_v, are introduced for later use.

2.2 Micro Actuator (MA)

As data densities in HDDs increase and track widths diminish, single-stage, conventional servo systems become less able to successfully position the head. A solution to these problems is to complement the VCM with a smaller, second actuator to form a dual-stage servo system. In this paper we consider the use of an MA, placed between the slider and the gimbal to create a translational in-plane rigid body motion of the slider relative to the suspension tip, which acts as a fine-positioning mechanism for the read/write head.

The input-output relation of the MA is expressed as

$$y_m(s) = G_m(s)(1 + W_m(s)\Delta(s))u_m(s) - \tilde{G}_m(s)y_v(s), \tag{3}$$

where u_m is the voltage to the MA and y_m is the generated slider motion, to be sensed with a capacitive sensor. The nominal model of the MA is assumed to be

$$G_m(s) := \frac{A_m}{s^2 + 2\zeta_m\omega_m + \omega_m^2}, \tag{4}$$

where A_m, ζ_m and ω_m are respectively the constant gain, the damping ratio and the natural frequency of the MA plant. Experimental results have verified that the transfer function in (4) accurately describes the dynamics of the MA [11]. However, because of fabrication variations, the parameters in (4) may vary from one MA to another. Therefore, we also assume that the MA dynamics in (3) has an uncertainty $W_m\Delta_m$, with $\|\Delta_m\|_\infty \leq 1$. Again, the variables (z_m, w_m) are introduced for later use. Finally, the term "$-\tilde{G}_m y_v$" in (3) is a coupling effect between the VCM and the MA which occurs when using a translational MA. The function $\tilde{G}_m$, which represents the dynamic coupling between the VCM input and the MA output, can be derived from (4) directly, and it has the form $\tilde{G}_m := s^2/(s^2 + 2\zeta_m\omega_m + \omega_m^2)$[1].

2.3 Runout

The track runout r, which is caused by various sources, is assumed to be lumped and modeled as

$$r(s) := W_r(s)w_r(s), \tag{5}$$

where w_r is white noise with Gaussian distribution and W_r is a shaping filter. The read/write head located in the slider measures its position $y_h := y_v + y_m$, relative to the track runout, and generates the PES

$$y_{pes} := r - y_h, \tag{6}$$

every time the slider flies over a servo sector region on the disk. The variance of this signal should be kept small for good track-following.

[1] $\tilde{G}$ is set to zero if the MA is rotational.

2.4 Measurements

There are three measurements in our multi-sensing system: $\hat{y}_{pes} := y_{pes} + n_{pes}$, $\hat{y}_p := y_p + n_p$ and $\hat{y}_m := y_m + n_m$, where "n" denotes the measurement white noise with Gaussian distribution. The PES $\hat{y}_{pes}$ is assumed to be measured with a 25kHz sampling rate, while the sampling rate of the other two signals is assumed to be 50kHz, twice as fast as that of $\hat{y}_{pes}$.

To sum up this section, the DSMS system that we consider in this paper can be regarded as a black-box, having white noise disturbances $(w_r, w_a, n_{pes}, n_p, n_m)$, control inputs (u_v, u_m), and measurements $(\hat{y}_{pes}, \hat{y}_p, \hat{y}_m)$ (see Figure 2).

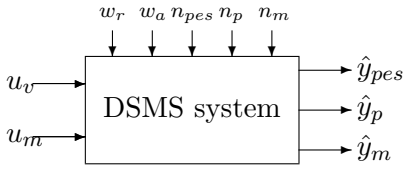

Figure 2: Inputs and outputs of the DSMS system

3 Robust multi-rate track-following controller design

For the DSMS system described in Section 2, we will formulate a robust track-following problem as follows: Design a discrete-time controller K which has three inputs $(\hat{y}_{pes}, \hat{y}_p, \hat{y}_m)$ and two outputs (u_v, u_m) such that

- the PES has a small RMS value, and
- the closed-loop system is robustly stable for uncertainties Δ_v and Δ_m, as well as parametric uncertainties in G_v and G_m.

Next, we shall provide a procedure to design a controller which solves this problem "approximately," in the sense that we ignore the inter-sampling behavior and that the procedure only guarantees robust stability for individual, not simultaneous, dy-

namic perturbations. After the design, we will test robust stability for parametric variations in G_v and G_m.

3.1 A generalized plant

First, we construct a continuous-time generalized plant, which reflects the robust track-following problem as depicted in Figure 3, by extracting the uncertainties and by connecting a discrete-time controller $K(z)$ with a multi-rate sampler S and a zero-order hold H.

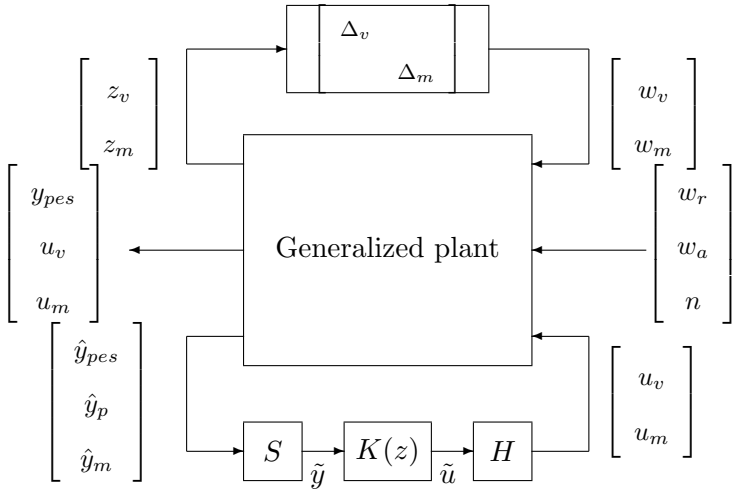

Figure 3: A generalized plant with an uncertainty block and a controller: Notation for signals are given in Section 2, $n := [n_{pes}, n_p, n_m]^T$, and $(\tilde{u}, \tilde{y})$ will be introduced in Section 3.2.

Although our main goal is to obtain a small y_{pes}, we have included (u_v, u_m) in the controlled output channel, to impose constraints on input magnitudes.

3.2 Derivation of a periodically time-varying system

Next, we discretize the generalized plant by using the zero-order hold with a sampling rate of 50kHz:

$$\begin{bmatrix} x(k+1) \\ z_\infty(k) \\ z_2(k) \\ y(k) \end{bmatrix} = \begin{bmatrix} A & B_\infty & B_2 & B_u \\ C_\infty & D_{\infty\infty} & D_{\infty 2} & D_{\infty u} \\ C_2 & D_{2\infty} & D_{22} & D_{2u} \\ C_y & D_{y\infty} & D_{y2} & 0 \end{bmatrix} \begin{bmatrix} x(k) \\ w_\infty(k) \\ w_2(k) \\ u(k) \end{bmatrix}, \tag{7}$$

where x is the discrete-time state of the generalized plant,

$$\begin{aligned} z_\infty &:= [z_v, z_m]^T, & w_\infty &:= [w_v, w_m]^T, \\ z_2 &:= [y_{pes}, u_v, u_m]^T, & w_2 &:= [w_r, w_a, n]^T, \\ y &:= [\hat{y}_{pes}, \hat{y}_p, \hat{y}_m]^T, & u &:= [u_v, u_m]^T, \end{aligned} \tag{8}$$

and all the matrices are defined as transfer matrices between the corresponding channels. (The meaning of the subscripts "∞" and "2" will become clear later.)

Now, following the technique used in [9], the multi-rate sampler S can be written mathematically as

$$S : \tilde{y}(k) = \Gamma(k) y(k), \quad k = 0, 1, 2, \ldots, \tag{9}$$

where $\{\Gamma(k)\}_{k\geq 0}$ is a sequence of matrices defined by

$$\left\{ \Gamma(k) := \left\{ \begin{array}{ll} I_3, & \text{if } k \text{ is even} \\ \begin{bmatrix} 0 & 0 \\ 0 & I_2 \end{bmatrix}, & \text{if } k \text{ is odd} \end{array} \right\}_{k\geq 0} \right. . \tag{10}$$

The sequence $\{\Gamma(k)\}_{k\geq 0}$ captures the multi-rateness of our problem; at even times, we sample all the measurements, while at odd times, we cannot measure $\hat{y}_{pes}$ because of its slow sampling rate. Similarly, we can express the hold H as

$$H : u(k) = \Omega(k) \tilde{u}(k), \quad k = 0, 1, 2, \ldots, \tag{11}$$

where we take $\Omega(k) = I_2$ for all k. This means that we send both control signals at the fast sampling rate of 50kHz, in order to achieve high track-following performance of the closed-loop system.

Combining the sampler S and the hold H with the discretized generalized plant results in the following periodically time-varying generalized plant:

$$\begin{bmatrix} x(k+1) \\ z_\infty(k) \\ z_2(k) \\ \tilde{y}(k) \end{bmatrix} = \begin{bmatrix} A & B_\infty & B_2 & B_u \\ C_\infty & D_{\infty\infty} & D_{\infty 2} & D_{\infty u} \\ C_2 & D_{2\infty} & D_{22} & D_{2u} \\ \Gamma(k)C_y & \Gamma(k)D_{y\infty} & \Gamma(k)D_{y2} & 0 \end{bmatrix} \begin{bmatrix} x(k) \\ w_\infty(k) \\ w_2(k) \\ \tilde{u}(k) \end{bmatrix}. \tag{12}$$

In our case, this plant is periodically time-varying with period 2.

3.3 A mixed H_2/H_∞ control problem for the periodically time-varying system

For the system (12), we formulate an optimization problem which reflects our control problem as follows:

$$\min_K \gamma_0 \quad \text{subject to} \begin{cases} K \text{ stabilizes the nominal system,} \\ \|T_{z_2 w_2}\|_2 < \gamma_0 \\ \left\|e_i^T T_{z_\infty w_\infty} e_i\right\|_\infty < \gamma_i, \quad i = 1, 2, \end{cases} \tag{13}$$

where T_{qp} denotes the map from the channel p to the channel q, e_i is the i-th unit vector, and γ_i is a positive scalar to be tuned by the designer.

We remark that the norms used in (13) are for time-varying systems. The norm $\|\cdot\|_2$ is a generalization of the standard H_2 norm to a norm for time-varying systems, and is defined in [13, page 73]. On the other hand, the norm $\|\cdot\|_\infty$ in (13) is used with an abuse of notation; it means the ℓ_2-induced norm. We use this notation to emphasize that this optimization is a generalization of the standard mixed H_2/H_∞

optimization for time-invariant cases to that for time-varying cases. Roughly speaking, the minimization of $\|T_{z_2 w_2}\|_2$ corresponds to the minimization of the RMS value of the PES, while the norm constraints on $\left\|e_i^T T_{z_\infty w_\infty} e_i\right\|_\infty$ lead to robust stability against plant uncertainties Δ_v and Δ_m.

Remarkable results in [13, 3, 9] proved that many important control synthesis problems for time-varying systems can be solved in a very similar way to those for time-invariant systems. Moreover, for periodically time-varying systems, these problems can be reduced to finite-dimensional convex optimization problems, which can be solved by using linear matrix inequalities (LMIs).

To be more concrete, using the matrices in the generalized plant (12), let us consider three auxiliary linear time-invariant systems having common input/output signals:

$$\begin{bmatrix} \boldsymbol{x}_2(k+1) \\ \boldsymbol{z}_2(k) \\ \boldsymbol{y}(k) \end{bmatrix} = \begin{bmatrix} Z\boldsymbol{A} & Z\boldsymbol{B}_2 & Z\boldsymbol{B}_u \\ \boldsymbol{C}_2 & \boldsymbol{D}_{22} & \boldsymbol{D}_{2u} \\ \boldsymbol{C}_y & \boldsymbol{D}_{y2} & 0 \end{bmatrix} \begin{bmatrix} \boldsymbol{x}_2(k) \\ \boldsymbol{w}_2(k) \\ \boldsymbol{u}(k) \end{bmatrix},$$

$$\begin{bmatrix} \boldsymbol{x}_\infty(k+1) \\ (\boldsymbol{z}_\infty)_i(k) \\ \boldsymbol{y}(k) \end{bmatrix} = \begin{bmatrix} Z\boldsymbol{A} & Z(\boldsymbol{B}_\infty)_i & Z\boldsymbol{B}_u \\ (\boldsymbol{C}_\infty)_i & (\boldsymbol{D}_{\infty\infty})_i & (\boldsymbol{D}_{\infty u})_i \\ \boldsymbol{C}_y & (\boldsymbol{D}_{y\infty})_i & 0 \end{bmatrix} \begin{bmatrix} \boldsymbol{x}_\infty(k) \\ (\boldsymbol{w}_\infty)_i(k) \\ \boldsymbol{u}(k) \end{bmatrix}, \quad i = 1, 2.$$

Here, the "shift" matrix Z is defined by

$$Z := \begin{bmatrix} 0 & I \\ I & 0 \end{bmatrix}, \tag{14}$$

and other matrices are block-diagonal[2] consisting of the matrices in (12); see the explicit forms of the matrices in Appendix. By a combination of the theories in [13, 3, 9], we can deduce the following equivalence:

[2]Throughout this paper, we use bold capital letters to denote block-diagonal matrices.

- A periodically time-varying controller

$$\begin{bmatrix} x_K(k+1) \\ \tilde{u}(k) \end{bmatrix} = \begin{bmatrix} K_A(k) & K_B(k) \\ K_C(k) & K_D(k) \end{bmatrix} \begin{bmatrix} x_K(k) \\ \tilde{y}(k) \end{bmatrix}, \tag{15}$$

  of period 2 solves the optimization problem (13),

- A time-invariant controller $\boldsymbol{K}$

$$\begin{bmatrix} \boldsymbol{x}_K(k+1) \\ \boldsymbol{u}(k) \end{bmatrix} = \begin{bmatrix} Z\boldsymbol{K}_A & Z\boldsymbol{K}_B \\ \boldsymbol{K}_C & \boldsymbol{K}_D \end{bmatrix} \begin{bmatrix} \boldsymbol{x}_K(k) \\ \boldsymbol{y}(k) \end{bmatrix}, \tag{16}$$

  solves the standard mixed H_2/H_∞ optimization problem for the system (14):

$$\begin{aligned} &\min_{\boldsymbol{K}} \gamma_0 \\ &\text{subject to} \begin{cases} \boldsymbol{K} \text{ stabilizes the nominal system,} \\ \|T_{\boldsymbol{z}_2\boldsymbol{w}_2}\|_2 < \sqrt{2\gamma_0^2} \\ \left\|T_{(\boldsymbol{z}_\infty)_i(\boldsymbol{w}_\infty)_i}\right\|_\infty < \gamma_i, \quad i = 1, 2, \end{cases} \end{aligned} \tag{17}$$

  Here, the matrices in (16) are block-diagonal defined by

$$\begin{aligned} \boldsymbol{K}_A &:= \begin{bmatrix} K_A(0) & 0 \\ 0 & K_A(1) \end{bmatrix}, \quad \boldsymbol{K}_B := \begin{bmatrix} K_B(0) & 0 \\ 0 & K_B(1) \end{bmatrix}, \\ \boldsymbol{K}_C &:= \begin{bmatrix} K_C(0) & 0 \\ 0 & K_C(1) \end{bmatrix}, \quad \boldsymbol{K}_D := \begin{bmatrix} K_D(0) & 0 \\ 0 & K_D(1) \end{bmatrix}, \end{aligned} \tag{18}$$

  and the block sizes in Z are compatible with the block sizes in $\boldsymbol{K}_A$.

The latter problem (17) is numerically solvable via the solution of LMIs for the time-invariant mixed H_2/H_∞ optimization; see for example [14, 12] and references therein. The LMIs that we have used to solve (17), as well as the construction of a periodically time-varying controller in (15), are shown in the Appendix.

Remark 3.1 In this section, we have just considered the case where the ratio of the faster sampling/hold rates to the slower one is two. However, it is straightforward to

extend the discussions in this section to a general case where the ratio is any natural number. Thus, if the ratio is N, then the resulting controller will be periodically time-varying with period N. We can expect that the larger this ratio becomes, the better the performance will be. However, as N increases, the number of decision variables and matrix inequalities increases drastically in the solution of the associated LMIs, and also the realization of the controller in the computer becomes more complex and computationally demanding.

4 Analysis of the designed controller: Simulation study

Using the DSMS system and the design procedure described in previous sections, we can design a multi-rate track-following controller. To obtain a low-order controller, during the controller design, we have used a model which is simpler than G_v in (2) but captures the major resonance modes of G_v. However, for the analysis of the designed controllers, we use the full order model G_v.

The order of the designed periodically time-varying controller was 13. To evaluate the effectiveness of the multi-rate controller, we have also designed a single-rate controller, in which all output signals are sampled with the same 25kHz rate as the PES. For comparison, we have set the same robust stability constraints, γ_1, γ_2 in (17), during both the multi-rate and single-rate designs. For the single-rate case, the controller is time-invariant, and the order of the controller is also 13.

First, time domain simulations have been done for both controllers. The PES signals are shown in Figure 4, where we can notice that the multi-rate controller achieves a smaller RMS value than its single rate counter part. This is also confirmed by the PES RMS values shown in Table 1. As can be seen in both the figures and the table, the track-following property can be greatly (about 30%) improved by using the multi-rate controller, with the same guaranteed robust stability margin. This illustrates the efficiency of the multi-rate controller for track-following.

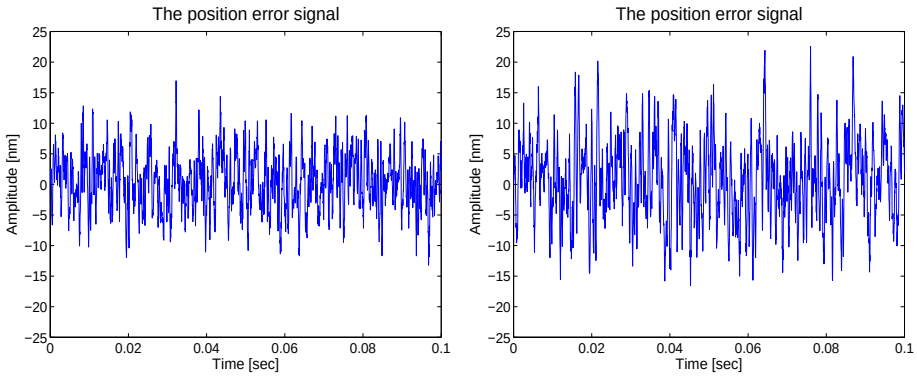

Figure 4: The position error signals for the multi-rate controller (left figure) and for the single-rate controller (right figure).

		RMS of PES (nm)
Mixed H_2/H_∞	Multi-rate	4.414
	Single-rate	6.274
LQG	Multi-rate	1.3659
	Single-rate	2.1958

Table 1: Comparison of RMS values of the PES for the multi-rate and the single-rate controllers

Next, we test the robustness of the controllers. Since G_v and G_m respectively have 7 modes and 1 mode, and since each mode is specified by 3 (i.e., (A, ζ, ω)) parameters, there are 24 parameters in total. We assume variations of these 24 parameters. The ranges of the variations with respect to nominal values are shown in Table 2. We have randomly generated, 1000 times, the 24 parameters within the ranges in Table 2, and checked how many times the multi-rate mixed H_2/H_∞ controller and the multi-rate H_2 (LQG) controller stabilize the closed-loop system. A simulation result is shown in Table 3, where one can see that the multi-rate mixed H_2/H_∞ controller is significantly more robust than the multi-rate LQG controller.

	A	ζ	ω
G_v	5%	20%	8%
G_m	5%	20%	12%

Table 2: Parameter variation ranges in G_v and G_m

Controller	# of stabilized cases
Mixed H_2/H_∞	956/1000
LQG	648/1000

Table 3: Robustness test

Remark 4.1 For design purposes, we modeled the uncertainties (Δ_v and Δ_m) as dynamic unstructured ones, while we have assumed parameter uncertainties to check system robustness, which is more realistic and less conservative. Obviously, there is a gap between these two types of uncertainties. To incorporate parameter variations in the design, we need to solve a discrete-time periodically time-varying version of robust H_2 synthesis.

5 Conclusions

In this paper, we have proposed a new design method for robust track-following controllers in HDDs. To achieve high tracking performance, we have assumed a dual-stage multi-sensing servo system, as well as multi sampling rates. The design problem has been reduced to a periodically time-varying version of the mixed H_2/H_∞ control problem, and solved by LMIs. A simulation study has shown that multi-rate mixed H_2/H_∞ controllers can drastically improve the track-following performance compared to single-rate controllers, while still maintaining robust stability.

There are several related subjects which are under investigation. As for the

design, the inter-sampling behavior, which is ignored in the current paper, should be incorporated. This would be accomplished by using the concept of "jump system" in [2, 9]. In addition, it will be better to take into account parametric variations in the multi-rate robust H_2 design. Moreover, after the design of periodically time-varying controllers, controller order reduction may be necessary. As for analysis, frequency domain μ-type analysis for robust stability and robust performance for periodically time-varying systems would be useful in evaluating the designed controllers. These are the future research topics.

A LMIs for discrete-time time-varying mixed H_2/H_∞

For completeness, we give the LMIs that were used for solving the optimization problem (17). These LMIs can be derived by combining the ideas of congruent transformations in [14] and of synthesis for time-varying systems in [3, 13]. We use the notation

$$
\begin{aligned}
&\boldsymbol{A} := I_2 \otimes A, && (\boldsymbol{B}_\infty)_i := I_2 \otimes B_\infty e_i,\\
&\boldsymbol{B}_2 := I_2 \otimes B_2, && \boldsymbol{B}_u := I_2 \otimes B_u,\\
&(\boldsymbol{C}_\infty)_i := I_2 \otimes (e_i^T C_\infty)/\gamma_i, && \boldsymbol{C}_2 := I_2 \otimes C_2,\\
&\boldsymbol{C}_y := \begin{bmatrix} \Gamma(0)C_y & 0 \\ 0 & \Gamma(1)C_y \end{bmatrix}, && (\boldsymbol{D}_{\infty\infty})_i := I_2 \otimes (e_i^T D_{\infty\infty} e_i)/\gamma_i,\\
&(\boldsymbol{D}_{\infty u})_i := I_2 \otimes (e_i^T D_{\infty u})/\gamma_i, && \boldsymbol{D}_{22} := I_2 \otimes D_{22},\\
&\boldsymbol{D}_{2u} := I_2 \otimes D_{2u}, && (\boldsymbol{D}_{y\infty})_i := \begin{bmatrix} \Gamma(0)D_{y\infty}e_i & 0 \\ 0 & \Gamma(1)D_{y\infty}e_i \end{bmatrix},\\
&\boldsymbol{D}_{y2} := \begin{bmatrix} \Gamma(0)D_{y2} & 0 \\ 0 & \Gamma(1)D_{y2} \end{bmatrix},
\end{aligned}
$$

where $\otimes$ denotes the Kronecker product. Notice that the number of blocks corresponds to the period of the original time-varying system (12). Additionally, for a

block-diagonal matrix $\boldsymbol{M}$ and a shift matrix Z (see (14)) with appropriate block sizes, we define

$$\boldsymbol{M}_Z := Z^T \boldsymbol{M} Z. \tag{19}$$

Note that $\boldsymbol{M}_Z$ is also block-diagonal.

To solve (17), we solve the following optimization with LMIs with respect to block-diagonal symmetric matrices $\boldsymbol{W}, \boldsymbol{X}, \boldsymbol{Y}$ and block-diagonal general matrices $\hat{\boldsymbol{K}}_A, \hat{\boldsymbol{K}}_B, \hat{\boldsymbol{K}}_C, \hat{\boldsymbol{K}}_D$ of appropriate dimensions:

$$\min \mathrm{trace} \boldsymbol{W}, \tag{20}$$

subject to

$$\begin{bmatrix} \boldsymbol{W} & \boldsymbol{C}_2 + \boldsymbol{D}_{22}\hat{\boldsymbol{K}}_D\boldsymbol{C}_y & \boldsymbol{C}_2\boldsymbol{Y} + \boldsymbol{D}_{2u}\hat{\boldsymbol{K}}_C & \boldsymbol{D}_{22} + \boldsymbol{D}_{2u}\hat{\boldsymbol{K}}_D\boldsymbol{D}_{y2} \\ * & \boldsymbol{X} & I & 0 \\ * & * & \boldsymbol{Y} & 0 \\ * & * & * & I \end{bmatrix} > 0,$$

$$\begin{bmatrix} \boldsymbol{X}_Z & I & \boldsymbol{X}_Z\boldsymbol{A} + \hat{\boldsymbol{K}}_B\boldsymbol{C}_y & \hat{\boldsymbol{K}}_A & \boldsymbol{X}_Z\boldsymbol{B}_2 + \hat{\boldsymbol{K}}_B\boldsymbol{D}_{y2} \\ * & \boldsymbol{Y}_Z & \boldsymbol{A} + \boldsymbol{B}_u\hat{\boldsymbol{K}}_D\boldsymbol{C}_y & \boldsymbol{A}\boldsymbol{Y} + \boldsymbol{B}_y\hat{\boldsymbol{K}}_C & \boldsymbol{B}_2 + \boldsymbol{B}_u\hat{\boldsymbol{K}}_D\boldsymbol{D}_{y2} \\ * & * & \boldsymbol{X} & I & 0 \\ * & * & * & \boldsymbol{Y} & 0 \\ * & * & * & * & I \end{bmatrix} > 0,$$

$$
\left[\begin{array}{ccccc}
\boldsymbol{X}_Z & I & \boldsymbol{X}_Z\boldsymbol{A}+\hat{\boldsymbol{K}}_B\boldsymbol{C}_y & \hat{\boldsymbol{K}}_A & \boldsymbol{X}_Z(\boldsymbol{B}_\infty)_i+\hat{\boldsymbol{K}}_B(\boldsymbol{D}_{y\infty})_i \\
* & \boldsymbol{Y}_Z & \boldsymbol{A}+\boldsymbol{B}_u\hat{\boldsymbol{K}}_D\boldsymbol{C}_y & \boldsymbol{A}\boldsymbol{Y}+\boldsymbol{B}_u\hat{\boldsymbol{K}}_C & (\boldsymbol{B}_\infty)_i+\boldsymbol{B}_u\hat{\boldsymbol{K}}_D(\boldsymbol{D}_{y\infty})_i \\
* & * & \boldsymbol{X} & I & 0 \\
* & * & * & \boldsymbol{Y} & 0 \\
* & * & * & * & I \\
* & * & * & * & *
\end{array}\right.
$$

$$
\left.\begin{array}{c}
0 \\
0 \\
(\boldsymbol{C}_\infty)_i^T+\boldsymbol{C}_y^T\hat{\boldsymbol{K}}_D^T(\boldsymbol{D}_{\infty u})_i^T \\
\boldsymbol{Y}(\boldsymbol{C}_\infty)_i^T+\hat{\boldsymbol{K}}_C^T(\boldsymbol{D}_{\infty u})_i^T \\
(\boldsymbol{D}_{\infty\infty})_i^T+(\boldsymbol{D}_{y\infty})_i^T\hat{\boldsymbol{K}}_D^T(\boldsymbol{D}_{\infty u})_i^T \\
I
\end{array}\right] > 0.
$$

Note that all the entries in the above LMIs are block-diagonal. For the controller construction, we first compute block-diagonal nonsingular matrices $\boldsymbol{M}$ and $\boldsymbol{N}$, having the same block structure as $\boldsymbol{X}$ and $\boldsymbol{Y}$, and satisfying

$$\boldsymbol{M}\boldsymbol{N}^T = I - \boldsymbol{X}\boldsymbol{Y}. \tag{21}$$

The controller matrices are given by

$$\boldsymbol{K}_D = \hat{\boldsymbol{K}}_D, \tag{22}$$

$$\boldsymbol{K}_C = (\hat{\boldsymbol{K}}_C - \hat{\boldsymbol{K}}_D\boldsymbol{C}_y\boldsymbol{Y})\boldsymbol{N}^{-T}, \tag{23}$$

$$\boldsymbol{K}_B = \boldsymbol{M}_Z^{-1}(\hat{\boldsymbol{K}}_B - \boldsymbol{X}_Z\boldsymbol{B}_2\hat{\boldsymbol{K}}_D), \tag{24}$$

$$\begin{aligned}\boldsymbol{K}_A = \boldsymbol{M}_Z^{-1}\Big\{&\hat{\boldsymbol{K}}_A - \boldsymbol{X}_Z(\boldsymbol{A}+\boldsymbol{B}_u\hat{\boldsymbol{K}}_D\boldsymbol{C}_y)\boldsymbol{Y} \\ &-\boldsymbol{X}_Z\boldsymbol{B}_u\boldsymbol{K}_C\boldsymbol{N}^T - \boldsymbol{M}_Z\boldsymbol{K}_B\boldsymbol{C}_y\boldsymbol{Y}\Big\}\boldsymbol{N}^{-T}.\end{aligned} \tag{25}$$

Note that the block structures of $\boldsymbol{K}_A$, $\boldsymbol{K}_B$, $\boldsymbol{K}_C$ and $\boldsymbol{K}_D$ are guaranteed in the computations, since all the matrices in the right-hand sides of (22)–(25) are block-diagonal. The corresponding periodically time-varying controller can be obtained by dividing these block matrices as in (18).

Acknowledgment

This research was supported by the Information Storage Industry Consortium (INSIC), the Computer Mechanics Laboratory (CML) at UC Berkeley and the Swedish Research Council (VR).

References

[1] T. Chen and L. Qui. H_∞ design of general multi-rate sampled-data control systems. *Automatica*, 30(7):1139–1152, 1994.

[2] G. E. Dullerud and S. Lall. Asynchronous hybrid systems with jumps – analysis and synthesis methods. *Systems and Control Lett.*, 37(2):61–69, 1999.

[3] G. E. Dullerud and S. Lall. A new approach for analysis and synthesis of time-varying systems. *IEEE Trans. Automat. Control*, 44(8):1486–1497, August 1999.

[4] P. Gahinet and P. Apkarian. A linear matrix inequality approach to H_∞ control. *Int. J. Robust and Nonlinear Control*, 4:421–448, 1994.

[5] P. Gahinet, A. Nemirovske, A. J. Laub, and M. Chilali. *LMI Control Toolbox*. The MathWorks, Inc., USA, 1995.

[6] M. Hirata, M. Takiguchi, and K. Nonami. Track-following control of hard disk drives using multi-rate sampled-data H_∞ control. In *Proceedings of the 42nd IEEE Conference on Decision and Control*, pages 3414–3419, Maui, Hawaii, 2003.

[7] R. Horowitz, T. L. Chen, K. Oldham, and Y. Li. Design, fabrication and control of micro-actuator for dual-stage servo systems. Springer Handbook of Nanotechnology, January 2004. Edit. Bharat Bushan.

[8] X. Huang, R. Nagamune, R. Horowitz, and Y. Li. Design and analysis of a dual-stage disk drive servo system using an instrumented suspension. In *Proc. of Amer. Control Conf.*, volume 4, pages 535–540, 2004.

[9] S. Lall and G. Dullerud. An LMI solution to the robust synthesis problem for multi-rate sampled-data systems. *Automatica*, 37(12):1909–1922, 2001.

[10] Y. Li, F. Marcassa, R. Horowitz, R. Oboe, and R. Evans. Track-following control with active vibration damping of a PZT-actuated suspension dual-stage servo system. In *Proc. of Amer. Control Conf.*, volume 3, 2003.

[11] K. Oldham, X. Huang, A. Chahwan, and R. Horowitz. Design, fabrication, and control of a high-aspect ratio microactuator for vibration suppression in a hard disk drive. to be presented at the 2005 IFAC World Congress, Prague.

[12] M. C. D. Oliveira, J. C. Geromel, and J. Bernussou. Extended H_2 and H_∞ norm characterizations and controller parametrizations for discrete-time systems. *Int. J. Control*, 75(9):666–679, 2002.

[13] M. A. Peters and P. A. Iglesias. *Minimum entropy control for time-varying systems*. Systems & Control: Foundations & Applications. Birkhäuser, 1997.

[14] C. Scherer, P. Gahinet, and M. Chilali. Multiobjective Output-Feedback Control via LMI Optimization. *IEEE Trans. Automat. Control*, 42(7):896–911, July 1997.

[15] D. H. Shim, H. S. Lee, and L. Guo. Mixed-objective optimization of track-following controllers using linear matrix inequalities. In *Proc. of Amer. Control Conf.*, volume 3, pages 4323–4328, 2003.